Stability of ionizing shock waves in monatomic gases

M. Mond, I. Rutkevich, and E. Toffin
Department of Mechanical Engineering, Pearlstone Center for Aeronautical Engineering Studies, Ben-Gurion University, Beer-Sheva, Israel
(Received 14 April 1997)

The stability properties of strong shocks propagating in monatomic gases are investigated. The need for modification of the classical Dyakov-Kontorovich criteria for stability of shocks rose as the straightforward application of the latter failed to explain the accumulating observations of irregular behavior behind strong shocks. In the current work, it is shown that the thermal nonequilibrium between the electrons that are produced by the electron-atom ionization process and the remaining atoms and ions plays a decisive role in the onset of a particular type of instability, namely, spontaneous emission. For that purpose, a two-fluid model is constructed in order to describe those perturbations whose frequencies are high enough so that a difference between the temperatures of the electrons, atoms, and ions may be maintained over a single period of the perturbations. Within the framework of this model, the energy losses due to the excitations of the electronic levels of the atoms as well as the ionization processes are taken into account. The two-fluid model allows the reformulation of the stability criterion in order to take into account the electronic temperature, as follows from the dominance of the electron-atom collisions in the ionization processes. In addition, the sound velocity, which plays an important role in calculating the stability criteria, is derived for the two-fluid system. It is shown that the modified criterion for spontaneous emission from the shock's front is satisfied for Mach numbers beyond a certain threshold. Furthermore, it is shown that the main mechanism for that instability is provided by the single ionization process, whereas the excitations of the electronic energy levels result in a slight modification of the instability threshold. A parametric study is carried out in order to find the domains in parameter space in which spontaneous emission occurs. It is shown that the parameters of available experiments that exhibit irregular behavior behind strong shocks do indeed fall within the theoretical domains of spontaneous emission. [S1063-651X(97)11511-2]

PACS number(s): 52.35.Tc, 47.40.−x, 83.50.Jf

I. INTRODUCTION

Interest in hypersonic flow has risen dramatically since the transition to supersonic flights in the early 1960s. Thus modern day space shuttle reenter the Earth's atmosphere at Mach 25 and further space missions are planned for speeds as high as Mach 50 [1]. Unlike supersonic flow, within the hypersonic regime various physical processes become progresively important as the flow velocity as well as the temperature increases to higher values. Of particular importance and interest are the properties of the flow behind strong shock waves. The latter may appear either ahead of a hypersonically moving body or attached to its contour lines. When the shock's Mach number is high enough, the flow behind it is hypersonic at high temperature and hence significantly influenced by such real gas effects as excitations of electronic levels of the atoms, dissociations, and ionizations [1–3].

Over the last decades the interest in hypersonic, high-temperature, flows and in particular in high Mach number shock waves has considerably expanded beyond the flight applications and is now embracing a wide range of issues of technological as well as of fundamental nature. Thus one may point out the use of shock-heated gases as a source of UV [4], the shock wave formation of supersonic plasma jets for propulsion [5], and the acceleration of small projectile using the ram concept [6]. On the other hand, high Mach number shock waves may play an important role in theoretical physics. In astrophysics, for example, high Mach number shock waves may provide an invaluable information about phenomena ranging from the chemical composition of large meteorites during their atmospheric entry [7], through the distribution of radiation sources in stellar atmospheres and wind [8], and to the determination of the structure of interstellar and intergalactic matter [9].

A deep interest in the problem of shock waves instabilities has risen during the last two decades due to some experimental evidence of irregular features of the flow behind strong ionizing and dissociating shocks [10–14]. The problem of shock wave instability belongs to the fundamental problems of fluid mechanics alongside with the Rayleigh-Taylor and the Kelvin-Helmholtz instabilities. Unlike the latter whose linear stages were well investigated and understood as early as the 19th century, the criteria for shock waves instability were first derived only in 1954 by Dyakov [15] who formulated the problem of corrugation instability of the shock's front. Under such an instability, sinusoidal deformation of the initially planar shock front grows exponentially in time. In addition, Dyakov and later on Kontorovich [16,17] have also found the circumstances under which small acoustic and entropy-vortex perturbations are emitted from the shock's front. That phenomenon was termed *spontaneous emission*. Even though the spontaneously emitted perturbations do not grow in time, their occurrence renders the flow behind the spontaneously emitting front unstable. This is due to the loss of the shock's energy that is continuously carried away by the outgoing waves and the subsequent reorganization of the initial flow.

Applying the Dyakov-Kontorovich criteria to shocks in a

perfect polytropic gas results in absolute stability, a not too surprising and a well-documented experimental fact. Furthermore, the straightforward employment of the Dyakov-Kontorovich criteria to strong ionizing shock has failed to explain the experimentally recorded instabilities [14,18]. As a result, various theories and models were constructed in order to understand the observed spatial oscillations in the mass density and in the electrons concentration behind strong enough shocks in monatomic gases [10,11]. Thus, Baryshnikov *et al.*, in a series of works (see, for example, [19]), suggested that even though the ionization process is endothermic, a sufficiently energetic intermediate exothermic stage may be responsible for the observed instability. Such a process was hypothesized to be the population of metastable electronic levels, above the atoms' thermal energy, due to atom-atom collisions and the subsequent release of the excess energy. Thus the released energy may amplify perturbations behind the shock. However, Houwing *et al.* [13] have shown experimentally that the proposed atom-atom collision mechanism for the creation of metastable states is not efficient enough and hence may not provide the explanation for the observed instabilities. Other attempts to explain the flow irregularities invoked the effects of dissipation processes such as viscous stress [20] and upstream radiation [21] on neutrally stable flows. However, no success was reported in finding neutrally stable flows, and hence the dissipation effects remained largely irrelevant. Recently, however, 20 years after their observation, the irregular features behind strong shocks were given theoretical explanation by Mond and Rutkevich [22]. In their work it was shown that the ionization by electron-atom collisions and the thermal nonequilibrium between the electrons and the heavy particles (e.g., atoms and ions) play a decisive role in the onset of spontaneous emission. Thus it was demonstrated that those perturbations are responsible for the observed irregularities whose frequencies allow the thermal nonequilibrium between the electrons and the heavy particles. Consequently, the classical Dyakov-Kontorovich criteria were modified with the aid of an appropriate two-fluid (electrons and heavy particles) model in order to account for the difference in the perturbed temperatures of the two species. Applying the modified criteria, it was shown that, indeed, strong ionizing shocks spontaneously emit acoustic as well as entropy-vortex waves as their Mach number crosses a certain threshold. The theoretical prediction of the latter was within reasonable agreement with the experimental observations in [10].

The goal of the present paper is twofold: to examine the effect of excitation of the electronic energy levels on the stability under spontaneous emission and to carry out a comprehensive parametric study that will shed light on the effects of various parameters such as the upstream pressure on the occurrence of spontaneous emission.

The structure of the paper is as follows: In Sec. II, the concept of unified shock is introduced and subsequently the Hugoniot curves are constructed for strong ionizing shocks. For that purpose the Saha equation for the degree of ionization is used as well as the Boltzman statistics for the excited electronic energy level. A numerical example of argon at room temperature is provided in order to demonstrate the general features of Hugoniot curves for strong shocks. Section III contains the analysis of the generalized conditions for spontaneous emission from shocks. It is shown that two ranges of frequencies exist for which the various inelastic processes behind the shock modify the classical Dyakov-Kontorovich criteria in a different manner. For one of the frequency ranges a two-fluid model of the gas behind the shock is constructed in Sec. IV. In Sec. V the criterion for spontaneous emission is examined numerically and a comprehensive study of domains of spontaneous emission in parameter space is carried out.

II. HUGONIOT CURVES FOR STRONG SHOCKS

The Hugoniot curves provide a viable tool for studying the steady-state as well as the stability properties of shock waves. Plotted in the P-η plane ($P=p_2/p_1$, $\eta=\rho_2/\rho_1$ are the pressure and density ratios across the shock, respectively), they represent all possible states, characterized by pressure p_2 and density ρ_2, behind a shock that propagates into a given gas at pressure pressure p_1 and density ρ_1. Furthermore, the shape of the Hugoniot curve plays a crucial role in determining the response of the steady-state flow induced by the shock to small perturbations. Therefore, the investigation of the properties of the Hugoniot curve is a necessary first step towards a comprehensive study of the shock's stability.

In the current work, a planar shock wave is considered that propagates into a cold, uniform, and unbounded monatomic gas. When the shock's Mach number M_1 is not too high, its width is of the order of few mean free paths and its Hugoniot curve is well known. In particular, the Hugoniot curve $\eta(P)$ is a monotonically increasing function that is bounded from above by the classical value of $(\gamma+1)/(\gamma-1)$, where γ is the specific heat ratio. However, as the shock's Mach number rises, so does the temperature behind it. Subsequently, inelastic processes such as excitation of the electronic energy levels in the atoms and the single and multiple ionization of the gas atoms and ions begin to play an increasingly important role in determining the flow properties behind the shock. Thus the classical gas-dynamical sharp shock gives way to a more complex flow pattern which is composed of four distinct areas (Fig. 1): (1) the region ahead of the shock in which the gas is in cold equilibrium (region 1), (2) the gas-dynamical shock, (3) the region along which the various inelastic processes are taking place, accompanied by a drop in the temperature and a consequent increase of the density (in this region neither dynamical nor thermal equilibrium is yet established and it is called in the literature the relaxation zone), and (4) the region in which a new equilibrium state is established and consequently all the physical variables maintain a constant value (region 2). Thus, for example, the concentration of electrons is zero right behind the gas-dynamical shock which marks the beginning of the relaxation zone and rises along it until it reaches a constant value at the verge of region 4. It should be noted that the flow variables in region 4 are only approximately constants due to the radiation from the hot gas in that region. However, the changes in the flow properties due to radiation occur over a length scale that is much longer than the relaxation zone and hence may be ignored.

The steady-state properties of the flow pattern of strong

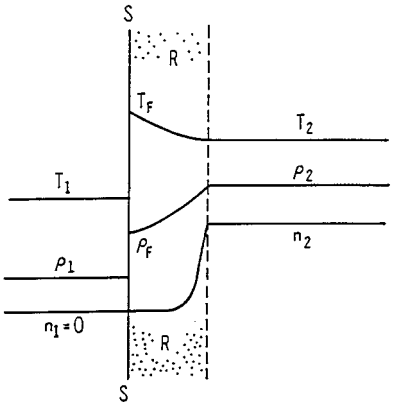

FIG. 1. A sketch of the behavior of the temperature T, the gas density ρ, and the electron concentration n in the vicinity of strong shocks. Subscripts 1, F, and 2 refer to upstream, frozen, and equilibrium states behind the shock, respectively. The relaxation zone is denoted by R.

shocks that were discussed above are traditionally investigated along two complementary parallel trends. Within the framework of the first one, the structure of the relaxation zone is studied. The rate equations for the various species are derived and integrated simultaneously with the gas-dynamical conservation laws along the relaxation zone. The end of the latter is determined when the gradients of the physical variables become sufficiently small [10,23–25]. This approach results in the profiles of the relevant physical quantities along the relaxation zone and hence enables the investigation of the dependence of its length on the gas properties ahead of the shock and on the shock's Mach number. In the current work the complementary approach is adopted in which the gas-dynamical shock together with the relaxation zone constitutes an effective surface of discontinuity that is treated as a single unified shock. It is this unified surface of discontinuity that will be meant from now on by the term ionizing shock. The properties of such shocks and in particular their Hugoniot curves, which significantly differ from their monotonically increasing classical counterparts, constitute the main interest of the current section.

The equations that describe the Hugoniot curve of the shocks are derived by writing the conservation equations that relate the two constant states on both sides of the shock. The flow is described in a frame of reference that is moving with the shock and hence $M_1>1$ and $M_2<1$. The continuity as well as the momentum equation have the same form as those for a classical gas-dynamical shock:

$$\rho_1 v_1=\rho_2 v_2=j, \tag{1}$$

$$p_1+jv_1=p_2+jv_2, \tag{2}$$

where v is the flow velocity. The energy equation, however, is modified due to the excitation and ionization processes and is given by

$$e_1+\frac{p_1}{\rho_1}+\frac{v_1^2}{2}=e_2+\frac{p_2}{\rho_2}+\frac{v_2^2}{2}+Q_{\rm ion}+Q_{\rm exc}, \tag{3}$$

where e is the internal energy per unit mass of the gas and $Q_{\rm ion}$ and $Q_{\rm exc}$ are the amounts of energy lost by the gas per unit mass due to ionization and excitation of electronic levels, respectively. The indices 1 and 2 denote the values of the parameters ahead of the shock (region 1) and behind it (region 2), respectively. The internal energy per unit mass is

$$e=\frac{p}{(\gamma-1)\rho}. \tag{4}$$

For a monatomic gas $\gamma=5/3$, and so this value will be used from now on. For single ionization processes, the energy-loss terms are

$$Q_{\rm ion}=\frac{\mathcal{N}I\alpha}{\mu}, \quad Q_{\rm exc}=\frac{\mathcal{N}\overline{E_a}(1-\alpha)}{\mu}, \tag{5}$$

where $\mathcal{N}$ is the Avogadro number, μ is the atomic weight of the gas, I is the ionization potential of the gas atoms, and E_a is the average electronic energy level. The ionization degree α is defined as

$$\alpha=\frac{n_e}{n_i+n_a}, \tag{6}$$

where n_e, n_i, and n_a are the concentrations of the free electrons, ions, and atoms, respectively. For single ionization, the equality $n_e=n_i$ is satisfied.

The total pressure in the mixture is the sum the partial pressures of the various species and is given by

$$p=kT(n_i+n_e+n_a), \tag{7}$$

where T is the temperature of the mixture. It should be noted that Eq. (7) is valid only in cases for which all species have the same temperature. Such is the case, for example, in the steady-state flow. However, as will be shown later on, when the flow is perturbed, not all species necessarily share the same temperature.

The average electronic energy level is calculated according to the Boltzmann statistics and is given by

$$\overline{E_a}(T)=\frac{1}{D_a}\sum_j g_a^j E_a^j \exp(-E_a^j/kT), \tag{8}$$

where D_a is the atoms' partition function and g_a^j and E_a^j are the degeneracy and the value of the jth energy level in the atoms, respectively. The partition function is

$$D_a=\sum_j g_a^j \exp(-E_a^j/kT). \tag{9}$$

The ionization degree α is calculated through the Saha equation

$$\frac{\alpha^2}{(1-\alpha)}=\frac{G}{(n_i+n_a)}\left[\frac{m_e kT}{2\pi\hbar^2}\right]^{3/2} e^{-I/kT}, \tag{10}$$

where $G=2D_i/D_a$, m_e is the electron's mass, and $\hbar$ is Planck's constant. The quantity D_i is the partition function of the single-charge ions and is calculated in an equivalent manner as in Eq. (9).

Equations (1)–(10) can be cast into a convenient form by defining the nondimensional variables

$$\eta=\frac{\rho_2}{\rho_1},\quad P=\frac{p_2}{p_1},\quad \theta=\frac{T_2}{T_1}, \tag{11}$$

in terms of which the Hugoniot curve, i.e., $\eta(P)$, is described by the implicit form

$$\eta(\theta)=\frac{1+4P(\theta)}{4+P(\theta)-\zeta\alpha(\eta(\theta),\theta)-\xi(\theta)[1-\alpha(\eta(\theta),\theta)]},$$

$$P(\theta)=[1+\alpha(\eta(\theta),\theta)]\theta\eta(\theta), \tag{12}$$

where

$$\zeta=\frac{2I}{kT_1},\quad \xi(\theta)=\frac{2\overline{E_a}(T)}{kT_1},$$

and α is

$$\alpha(\eta,\theta)=-\tfrac{1}{2}\psi+\sqrt{\tfrac{1}{4}\psi^2+\psi},$$

where

$$\psi=b(p_1,T_1)\,\theta^{3/2}\eta^{-1}e^{-\zeta/2\theta},$$

$$b(p_1,T_1)=G\left(\frac{m_e}{2\pi\hbar^2}\right)^{3/2}\frac{(kT_1)^{5/2}}{p_1}.$$

Typical values of ζ for $T_1=300$ K are of order 10^2 for alkali metal vapor and of 10^3 for inert gases. For example, for cesium and argon ζ is 301 and 1291, respectively. It should be noted that departure from the Saha equation due to radiation occurs only for high temperatures or low electronic concentrations [26], which is outside the range of parameters of interest in the current investigation. In addition, as is pointed out by Biberman *et al.* [28], the validity of the Saha equation implies the validity of the Boltzmann law for the distribution of electronic energy levels in the atoms, e.g., Eq. (8).

Before turning to the description of the Hugoniot curve, it is noticed that the infinite series on the right-hand sides of Eqs. (8) and (9) are divergent for free atoms. However, for atoms in a partially ionized plasma, only those levels should be taken into account whose orbital radius is smaller than the Debye radius [27,28]. Thus the infinite series in Eqs. (8) and (9) are truncated after a finite number of terms that is given by

$$N_{\max}=\left(\frac{Ir_D}{e^2}\right)^{1/2}, \tag{13}$$

where

$$r_D=\left(\frac{kT}{4\pi n_e e^2}\right)^{1/2}$$

is the Debye radius.

An example of a typical Hugoniot curve is presented in Fig. 2. The solid line displays the numerical solution of Eq. (12) for argon at $p_1=5$ Torr and $T_1=300$ K, while the dot-dashed line shows the Hugoniot curve without the effects of the excitation of the electronic levels. A detailed description of the main features of the Hugoniot curves of ionizing shocks may be found in Mond and Rutkevich [22]. Figure 2 reveals that taking into account the electronic excitation and calculating G more accurately leads to a very little change in the Hugoniot curve. Therefore, the steady-state properties of the ionizing shocks may be quite accurately calculated by the simpler model within which the electronic excitations are neglected and G is a constant. In particular, the use of that simpler model results in a universal law for the maximal degree of compression behind shocks propagating into cold inert gases [29].

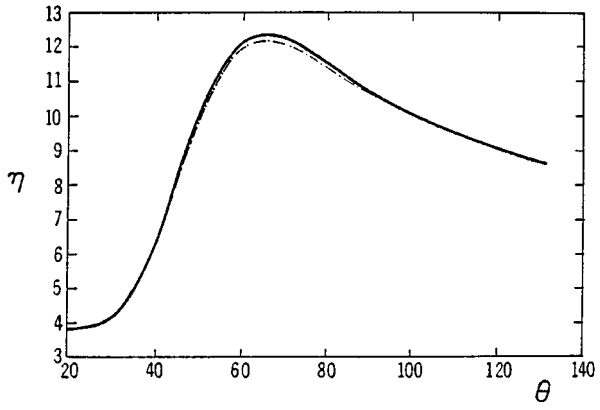

FIG. 2. The Hugoniot curve for argon at $T=300$ K and $p_1=5$ Torr. The solid line describes the Hugoniot curve with both ionization and electronic excitations, while the dot-dashed line includes only the effects of ionization.

III. GENERALIZED CONDITIONS FOR SPONTANEOUS EMISSION OF WAVES FROM SHOCKS

The problem of stability of shock waves has attracted the attention of researchers over the last 40 years, since Dyakov [15] formulated his conditions for the growth of the corrugation of the front of a shock that propagates with a constant velocity into a homogeneous unbounded medium. Dyakov's criterion, which was derived for an arbitrary equation of state, is

$$h<-1\quad\text{or}\quad h>1+2M_2, \tag{14}$$

where

$$h=-V_2^2\left(\frac{d\rho_2}{dp_2}\right)_H, \tag{15}$$

where V_2 is the flow velocity behind the shock (in the frame of reference that is moving with the shock), M_2 is the Mach number behind the shock, and $(d\rho_2/dp_2)_H$ is the slope of the Hugoniot curve. In addition, Dyakov and later on Kontorovich [15–17] have obtained the following condition for spontaneous emission of acoustic as well as entropy-vortex waves from the shock's front:

$$h_c<h<1+2M_2,\quad h_c=\frac{1-(\eta+1)M_2^2}{1+(\eta-1)M_2^2}. \tag{16}$$

Criterion (16) has been derived by Kontorovich by considering acoustic waves impinging on the shock front from behind. Since the flow ahead of the shock is supersonic (in the frame of reference that is moving with the shock), no wave is transmitted into that region. Thus the incident acoustic wave, having the form $\exp[i(k_x x+k_y y-\omega t)]$, gives rise to a reflected wave as well as an entropy-vortex wave, all of which propagate away from the shock in the region behind it. The entropy-vortex wave is created in order to satisfy the conservation laws on both sides of the corrugated shock front. The ratio of the reflected to incident acoustic-wave pressure amplitudes is the reflection coefficient. The spontaneous emission of acoustic (as well as entropy-vortex) waves from the shock's front occurs when the amplitude of the incident wave tends to zero while that of the reflected waves remains finite. In this limit the reflection coefficient tends to infinity.

Kontorovich was the first to correctly calculate the reflection coefficient. He derived a system of relations from which the latter may be obtained in terms of the angles between the various relevant directions that define the geometry of the physical system (for instance, the direction of propagation of the incident as well as of the reflected wave relative to the shock front). Recently, Mond and Rutkevich [22] have modified Kontorovich's approach and have introduced a frequency-dependent representation of the reflection coefficient. As will be shown later, such a representation is very useful and provides valuable insight when strong shocks are investigated that give rise to various inelastic processes each with its own time scale. In this case, the value of the waves' period relative to the various inelastic time scales plays a crucial role in determining the behavior of the physical system.

The reflection coefficient is obtained by linearizing the equations that describe the dynamics of the system and by using the Rankine-Hugoniot relations. For completeness, the expression for the reflection coefficient R is written below:

$$R=-\frac{f(q)-\sqrt{q^2-1}}{f(q)+\sqrt{q^2-1}}, \tag{17}$$

where

$$f=\frac{1-h}{2M_2}\,q-\frac{(1+h)\,\eta M_2}{2q(1-M_2^2)}, \quad q=\frac{\omega}{k_y c_2\sqrt{1-M_2^2}},$$

where k_y is the projection of the wave vector of the incident acoustic wave on the unperturbed shock plane and c_2 is the sound velocity behind the shock. In terms of the nondimensional parameters defined in the previous section the parameter h is

$$h=-\frac{j^2}{\rho_1 p_1 \eta^2}\left(\frac{\partial \eta}{\partial P}\right)_{\rho_1,p_1}. \tag{18}$$

Criterion (16) means that if it is satisfied, for any real value of ω a real value of k_y may be found such that the reflection coefficient is infinite and hence the shock spontaneously emits acoustic as well as entropy-vortex waves with those particular combinations of ω and k_y.

For gas-dynamic shocks, h is smaller than h_c for all values of the relevant physical parameters and hence classical shocks are stable under spontaneous acoustic emission. This result is certainly valid for shocks whose Mach numbers are not too high. Behind such shocks, the excitations of electronic levels as well as the ionization processes may be neglected. Consequently, M_2 is calculated by using the classical isoentropic sound speed in an ideal gas, while the parameter h is indeed proportional to the slope of the Hugoniot curve as is given by Eq. (18). However, this situation changes as the shock's Mach number increases so that various inelastic processes behind it play an increasingly important role in determining its properties. In particular, the emergence of different inelastic processes introduces into the system various characteristic time scales that are associated with them. As a result, the value of the frequency of the incident acoustic wave (which is also the frequency of the reflected as well as the entropy-vortex wave) relative to the various inelastic frequencies plays a decisive role in calculating the parameters for the stability criteria. Thus, as will be subsequently seen, the stability calculations should be modified in accordance with the particular properties of the perturbations within the relevant frequency domain. More specifically, a close inspection of the derivation of the stability criteria reveals that while the form of the criteria (14) and (16) remains unchanged, the parameters h and M_2 should be recalculated for each of the frequency domains that are defined by the various inelastic frequencies.

Deferring the calculation and discussion of the sound speed in kinetically active media to the next section, the attention is now focused on the calculation of h. This parameter is obtained from the relationship between the density and the pressure perturbation immediately behind the shock. A general expression for that purpose may be obtained through Eqs. (3)–(10) that can be symbolically written as

$$\begin{aligned}\rho_2&=\mathcal{F}(p_2,\alpha:\rho_1,p_1),\\ \alpha&=\mathcal{H}(T_2^e,\rho_2:\rho_1,p_1),\end{aligned} \tag{19}$$

where T_2^e is the temperature of the electrons. The reason that the ionization degree depends on the electrons' temperature is that the dominant ionization mechanism is the electron-atom impact. It should be noted here that in general the ionization processes are a result of a multitude of mechanisms. Thus, for example, for high temperatures or low electronic concentrations, photoionization may dominate [28]. However, for the range of parameters of interest in the current study, the effect of photoionization is negligible and the overall ionization process is dominated by collisions.

In steady state, under thermodynamic equilibrium $T_2^H=T_2^e=T_2$, where T_2^H is the temperature of the heavy particles (i.e., the atoms and the ions) and T_2 is a function of p_2 and ρ_2. As a result, Eqs. (19) represent the Hugoniot curve in the (ρ_2,p_2) plane. For time-dependent processes, however, thermal equilibrium between the electrons and the heavy particles may be violated. Furthermore, for time-dependent processes such as propagation of small perturbations, Eqs. (19) are appropriate only in a certain range of the perturbations frequencies. In particular, the first equation of Eqs. (19), which is the result of the integration of the con-

servation laws across the shock, was obtained by assuming that within the shock's width the terms that contain time derivatives in the conservation equations may be neglected relative to those containing spatial derivatives. In the classical gas-dynamic shocks, this certainly holds for any frequency since the shock's width is arbitrarily small and hence the spatial gradients are arbitrarily large in comparison with the time derivatives. However, for the model adopted in the current work, the ionizing shock is of finite width that is determined by the length of the relaxation zone. Hence the spatial gradients across the shock are finite. As a result, the steady-state relationship across the shock (i.e., across the relaxation zone) may be used for perturbations whose frequencies are small enough such that

$$\omega \ll \frac{V_2}{d}, \tag{20}$$

where d is the characteristic length for the variation of the density within the relaxation zone. It should be noted that in addition to condition (20) the model of a single surface of discontinuity is meaningful only for those perturbations whose wavelengths in the direction perpendicular to the shock's front are much bigger than the length of the relaxation zone.

Under condition (20) and taking into account the fact that the perturbations on the supersonic side of the shock are zero, Eqs. (19) may be used for the perturbed state

$$\rho_2+\delta\rho_2=\mathcal{F}(p_2+\delta p_2,\alpha+\delta\alpha;\rho_1,p_1), \tag{21}$$

which upon linearization results in

$$\frac{\delta\rho_2}{\delta p_2}=\left(\frac{\partial\rho_2}{\partial p_2}\right)_{\rho_1,p_1,\alpha}+\left(\frac{\partial\rho_2}{\partial\alpha}\right)_{\rho_1,p_1,p_2}\frac{\delta\alpha}{\delta p_2}. \tag{22}$$

The second term on the right-hand side of Eq. (22) is determined with the aid of the second equation in Eqs. (19), which expresses the balance between the sink and source terms in the rate equation for the electrons' concentration. This balance leads to the Saha equation and may be invoked for waves whose frequencies are much smaller than the inverse of the characteristic time for attaining ionization equilibrium. Since the latter is equal to $2\nu_{\rm ion}$, where $\nu_{\rm ion}$ is the ionization frequency, the Saha equation may be employed in order to calculate the perturbed electrons' concentration if

$$\omega \ll 2\nu_{\rm ion}. \tag{23}$$

The partial derivatives on the right-hand side of Eq. (22) are determined according to Eq. (12):

$$\left(\frac{\partial\rho_2}{\partial p_2}\right)_{\rho_1,p_1,\alpha}=\frac{\rho_1 q(1+\alpha)\eta+r}{p_1(1+\alpha)(\eta+r\theta)}, \tag{24}$$

$$\left(\frac{\partial\rho_2}{\partial\alpha}\right)_{\rho_1,p_1,p_2}=\rho_2\frac{s(1+\alpha)-r\theta}{(1+\alpha)(\eta+r\theta)}, \tag{25}$$

where

$$q=\frac{4}{D}-\frac{1+4P}{D^2},\quad s=q-\frac{4}{D},\quad r=s\frac{d\xi}{d\theta}(1-\alpha),$$

and

$$D=4+P-\zeta\alpha-\xi(1-\alpha),$$

where ζ and ξ are defined after Eq. (12). Unlike the partial derivatives in Eqs. (24) and (25), the manner of calculating the ratio of the ionization degree perturbation to the pressure perturbation, $\delta\alpha/\delta p_2$, depends on the frequency range of the perturbation. The low-frequency range is defined by $\omega \ll \nu_\epsilon$, where ν_ϵ is the inverse of the relaxation time of the heavy particles' temperature due to their collisions with electrons. In that low-frequency range the perturbations in the electrons' and the heavy particles' temperatures may be assumed to be equal, and a single-fluid model is appropriate for describing the propagation of small perturbations. Therefore,

$$\frac{\delta\alpha}{\delta p_2}=\left(\frac{\partial\alpha}{\partial p_2}\right)_{\rho_1,p_1}. \tag{26}$$

This means that the right-hand side of Eq. (22) is the total derivative along the Hugoniot curve. In this case h assumes its classical form given by Eq. (18).

For high enough frequencies such that $\omega \gg \nu_\epsilon$, the temperature perturbations of the electrons and the heavy particles cannot any longer be assumed to be equal. As a result, a two-fluid model that describes the perturbations in each of the components have to be invoked. For such perturbations, that in addition satisfy condition (23), $\delta\alpha/\delta p_2$ is calculated according to

$$\frac{\delta\alpha}{\delta p_2}=\left(\frac{\partial\alpha}{\partial T_2}\right)_{\rho}\frac{\delta T_2^e}{\delta p_2}+\left(\frac{\partial\alpha}{\partial\rho_2}\right)_{T}\frac{\delta\rho_2}{\delta p_2}. \tag{27}$$

As was explained before, the electrons' temperature is used in calculating $\delta\alpha/\delta p_2$ since for $\alpha > 10^{-3}-10^{-2}$ the dominant ionization mechanism is the electron-atom collision. As is obviously seen from Eq. (27), the calculation of the parameter h is now different from its classical definition as a derivative along the equilibrium Hugoniot curve. As will be seen in the next sections, it is those waves that belong to the higher-frequency range and are described by Eq. (27) that may become unstable under spontaneous emission of acoustic as well as entropy-vortex waves. It should be emphasized, though, that the size of such a frequency range, $\nu_\epsilon \ll \omega \ll 2\nu_{\rm ion}$, generally depends on the parameters of the gas ahead of the shock and on the latter's Mach number and for some range of parameters may altogether not exist. The conditions for the occurrence of such a frequency domain and its magnitude will be examined in the next sections.

To summarize, the generalized criterion for spontaneous acoustic emission from shocks is given by condition (16) in which the classical definitions of h and M_2 are modified due to the various inelastic processes behind strong shocks. The calculations of both h and M_2 depend on the value of the waves' periods relative to the time-scales of the various inelastic processes. Both functions, h and M_2, will be calculated in the next section.

IV. ACOUSTIC WAVES IN KINETICALLY ACTIVE MEDIA

In this section, the parameters h and M_2 that are needed for analyzing the conditions for spontaneous emission of acoustic and entropy-vortex waves from shocks are calculated for perturbations within the high-frequency regime discussed in the previous section. As was shown by Mond and Rutkevich [22], strong shocks are stable under spontaneous emission of waves whose frequencies are low enough so that thermal equilibrium is maintained between the electrons and the heavy particles. Hence the attention is focused on the high-frequency regime for which thermal equilibrium cannot be established during one wave's period. As is evident from the previous section, the single-fluid model is no longer adequate for the description of waves in that frequency range that is defined by $\nu_\epsilon \ll \omega \ll 2\nu_{\rm ion}$, which are propagating in the partially ionized gas behind strong shocks. Instead, a more complex model which consists of three components, namely, electrons, ions, and atoms, has to be employed. Even though all species have the same temperature in the equilibrium state behind the shock, their perturbed temperatures may differ from each other. However, simplifying the governing equations as much as possible while still preserving the physical phenomena of interest, it is assumed that the frequency of the acoustic oscillations, ω, is much smaller than both the effective frequencies of momentum as well as energy transfer between the ions and the atoms. As a result, the ions and the atoms share the same perturbed velocity, $\delta\mathbf{V}$, as well as the same perturbed temperature, δT. This assumption means that the ions and the atoms may be treated as a single fluid, the heavy-particles gas whose partial pressure is

$$p_H=(n_i+n_a)kT. \tag{28}$$

In addition, the partially ionized plasma behind the shock is assumed to be quasineutral. This assumption means that the perturbations in the concentrations of the electrons and the ions (δn_e and δn_i, respectively) are equal and is valid for waves whose period is much longer than the charge-separation relaxation time.

Waves that fulfill the above assumptions may be studied within the framework of a two-fluid model whose components are the electrons and the heavy particles. This model is characterized by the following linearized form of the conservation laws.

Conservation of the total number of the electrons:

$$\frac{\partial \delta n_e}{\partial t}+\boldsymbol{\nabla}\cdot(n_e\delta\mathbf{V}_e+\delta n_e\mathbf{V})=\delta\dot{n}_e, \tag{29}$$

where $\delta\dot{n}_e$ describes the perturbation in the source term in the rate equation for the electrons' concentration.

Conservation of the heavy-particles' mass:

$$\left(\frac{\partial}{\partial t}+\mathbf{V}\cdot\boldsymbol{\nabla}\right)\delta\rho+\rho\boldsymbol{\nabla}\cdot\delta\mathbf{V}=0 \tag{30}$$

Momentum equation for the heavy particles:

$$\left(\frac{\partial}{\partial t}+\mathbf{V}\cdot\boldsymbol{\nabla}\right)\delta\mathbf{V}=-\frac{\boldsymbol{\nabla}(\delta p_H+\delta p_e)}{\rho}. \tag{31}$$

In the collisional plasma behind the shock, the inertia of the electrons may be neglected in the equation that describes the conservation of their momentum. In that case, the electrons' momentum equation describes the balance between the electrons' pressure, the electric force and the momentum exchange with the heavy particles. Thus the last two may be expressed in terms of the electrons' pressure, δp_e, which now appears in the momentum conservation of the heavy particles, Eq. (31).

Energy equation for the electrons:

$$\left(\frac{\partial}{\partial t}+\mathbf{V}\cdot\boldsymbol{\nabla}\right)\left(\frac{3}{2}\,\delta p_e+I\delta n_e+\overline{E_a}\delta n_a+n_a\delta\overline{E_a}\right)$$
$$=\left(-\frac{5}{2}\,p_e-In_e-\overline{E_a}n_a\right)\boldsymbol{\nabla}\cdot\delta\mathbf{V}_e$$
$$-\frac{3m_e}{m_a}\,\nu_e k n_e(\delta T_e-\delta T), \tag{32}$$

where ν_e is the effective frequency of momentum transfer from the heavy particles to the electrons. The heavy-particle gas satisfies the adiabatic law

$$\frac{\delta p_H}{p_H}=\frac{5}{3}\,\frac{\delta\rho}{\rho}. \tag{33}$$

Equations (28)–(32) are supplemented by the Saha equation, which is satisfied due to the condition $\omega \ll 2\nu_{\rm ion}$ and according to Eq. (19) may be written as

$$\alpha+\delta\alpha=\mathcal{H}(T+\delta T_e,\rho+\delta\rho;T_1,\rho_1) \tag{34}$$

and by

$$\delta p=\delta p_e+\delta p_H. \tag{35}$$

As was discussed in Sec. II, the ionization degree is determined by the electronic temperature since the dominant ionization mechanism is the electron impact. In addition, since the Saha equation implies the validity of the Boltzmann statistics for atoms excited by electron impact, the perturbation of the average level of the electronic energy in the atoms is given by

$$\delta\overline{E_a}=\frac{d\overline{E_a}}{dT}\,\delta T_e. \tag{36}$$

An expression for the first term on the right-hand side of Eq. (32) may be obtained with the aid of the quasineutrality assumption which is expressed in the following way:

$$\boldsymbol{\nabla}\cdot en_e(\delta\mathbf{V}_e-\delta\mathbf{V})=0, \tag{37}$$

which results in

$$\boldsymbol{\nabla}\cdot\delta\mathbf{V}_e=\boldsymbol{\nabla}\cdot\delta\mathbf{V}. \tag{38}$$

The last term on the right-hand side of Eq. (32) expresses the energy exchange between the electrons and the heavy

particles. For ionizing shocks this term may be neglected relative to the second term on the right-hand side of Eq. (32) (energy loss due to ionization). The condition that enables such an approximation is

$$\frac{3m_e}{m_a}\frac{\nu_e}{\nu_{\rm ion}}\left(\frac{kT_e}{I}\right)^2 \ll 1. \tag{39}$$

When condition (39) is satisfied, Eq. (32) is reduced to

$$\frac{3}{2}\,\delta p_e + I\,\delta n_e + \overline{E_a}\,\delta n_a + n_a\,\delta\overline{E_a} = \left(\frac{5}{2}\,p_e + I n_e + \overline{E_a} n_a\right)\frac{\delta\rho}{\rho} \tag{40}$$

and the relationship between the pressure and density perturbations as calculated from Eqs. (29)–(33) is

$$\frac{\delta p}{p} = \gamma_{\rm eff}\frac{\delta\rho}{\rho}, \quad \gamma_{\rm eff} = \frac{5+3\alpha A}{3(1+\alpha)}, \tag{41}$$

where

$$A = \frac{\delta \ln p_e}{\delta \ln \rho} = \frac{5(1+\overline{\alpha_T}) + z'(\overline{\alpha_T} - \overline{\alpha_\rho}) + z_T(1+\overline{\alpha_\rho})}{3(1+\overline{\alpha_T}) + z'\overline{\alpha_T} + \tilde{z}}, \tag{42}$$

where

$$\overline{\alpha_T} = \left(\frac{\partial \ln\alpha}{\partial \ln T}\right)_\rho, \quad \overline{\alpha_\rho} = \left(\frac{\partial \ln\alpha}{\partial \ln\rho}\right)_T,$$

and

$$z' = \frac{2(I-\overline{E_a})}{kT}, \quad \tilde{z} = \frac{2}{k}\frac{d\overline{E_a}}{dT}\frac{1-\alpha}{\alpha}. \tag{43}$$

Through the definition of z', it is seen that the average excitation energy level acts as to effectively reduce the ionization potential.

Examining Eqs. (30), (31), and (35), it is clear that the sound speed behind the shock is

$$c_2 = \left(\gamma_{\rm eff}\frac{p_2}{\rho_2}\right)^{1/2}. \tag{44}$$

In order to complete the calculations needed for the stability analysis, the modified parameter h is derived. Thus using Eqs. (22) and (27) as well as Eqs. (29)–(41) results in

$$h = -\frac{j^2}{\rho_1 p_1 \eta^2}\left[\left(\frac{\partial\eta}{\partial P}\right)_{\rho_1,p_1,\alpha} + \frac{\alpha B}{P}\left(\frac{\partial\eta}{\partial\alpha}\right)_{\rho_1,P_1,P}\right], \tag{45}$$

where

$$B = \frac{[\overline{\alpha_T}(A-1) + \overline{\alpha_\rho}]}{\gamma_{\rm eff}(\overline{\alpha_T}+1)} \tag{46}$$

and the partial derivatives of η with respect to P and α are calculated from Eqs. (24) and (25).

To summarize, in order to determine the shock's stability under spontaneous acoustic emission, criterion (16) is used in which h is calculated according to Eq. (45), while the critical value h_c is determined by Eq. (16) in which the Mach number is

$$M_2^2 = \frac{\rho_2 V_2^2}{\gamma_{\rm eff}(\rho_2, T_2)p_2}. \tag{47}$$

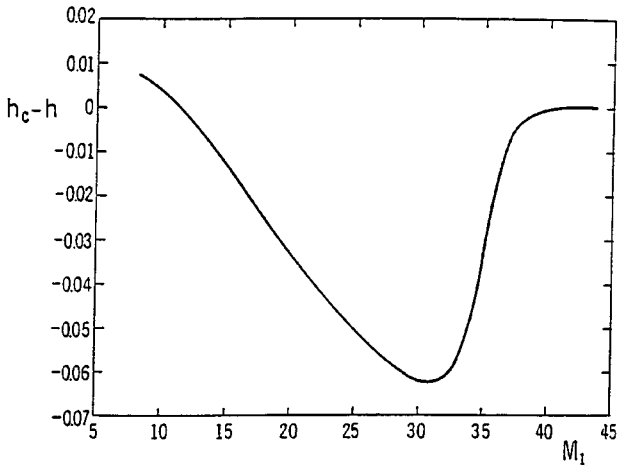

FIG. 3. The difference $h_c - h$ as a function of the temperature ratio behind the shock for ionizing shocks in argon at $T = 300$ K and $p_1 = 5$ Torr.

V. RESULTS AND DISCUSSION

In order to investigate the stability properties of strong shocks under spontaneous acoustic emission, numerical studies of inequalities (16) were carried out for the thermal nonequilibrium regime. Preliminary application of criterion (16) for waves in the frequency domain defined by $\nu_\epsilon \ll \omega \ll 2\nu_{\rm ion}$ demonstrated the occurrence of spontaneous emission for parameters that correspond to those used to experimentally observe irregularities behind strong shocks [11]. Thus h was calculated according to Eq. (45), while h_c was computed according to its definition in Eq. (16) in which the Mach number is given by expression (47) which holds for the kinetically active medium behind the shock. Both h and h_c were calculated along the Hugoniot curve [which is given by the solution of Eq. (12)] for various monatomic gases at a large variety of initial pressures. Results of a typical calculations are shown in Fig. 3, which depicts $h_c - h$ along the Hugoniot curve for argon at room temperature and initial pressure of 5 Torr. As can be seen, h becomes greater than h_c beyond a certain threshold, which means that ionizing shocks in argon spontaneously emit waves when their Mach number surpasses a certain value. According to the current calculations, as can be seen from Fig. 3, the critical Mach number is $M_{1c} \approx 12$. It should be noted that taking into account the excitation of the electronic levels of the argon atoms lowered slightly the threshold for spontaneous emission. This is so due to the reduced effective ionization potential as is expressed by z'. This result corresponds to the experimental observations of Glass and Liu [10]. In their experiments in argon at room temperature and $p_1 = 5$ Torr, they noticed that the regular shock structure of two constant states on both of its sides is disturbed for $M_1 > 14.7$. In that range of Mach

numbers, oscillations in the electron's concentration behind the shock was recorded by their interferograms. That and similar experiments in krypton [11] are in good qualitative as well as quantitative agreement with the present theoretical model.

Motivated by the correspondence between the predictions of the theoretical model and the experimental results, a comprehensive parametric study of the stability of strong shocks in argon at room temperature was carried out. The free parameters are the pressure p_1 ahead of the shock and the shock's Mach number M_1. Thus those domains in the (p_1,M_1) plane were found in which the shocks are unstable under spontaneous emission.

An important stage in finding the domains of spontaneous emission is the calculation of $\nu_{\rm ion}$ and ν_ϵ. Calculating the latter enables the determination of the domains in the (p_1,M_1) plane in which $2\nu_{\rm ion}\leqslant\nu_\epsilon$. Within those domains the simultaneous existence of thermal nonequilibrium and ionization equilibrium is impossible. Hence shocks propagating in gases that are characterized by such parameters are stable under spontaneous acoustic emission for $\omega\ll\nu_{\rm ion}$ or $\omega\gg\nu_\epsilon$ regardless of the formal calculation of h and h_c.

The expression for ν_ϵ is given by

$$\nu_e=2\frac{m_e}{m_a}\,\alpha(\nu_{ea}+\nu_{ei}), \tag{48}$$

where ν_{ea} and ν_{ei} are the elastic electron-atom and electron-ion collision frequencies, respectively. They are written in terms of the elastic cross section as follows [30]:

$$\nu_{ea}=\frac{(1-\alpha)\rho}{m_a}\left(\frac{8kT}{\pi m_e}\right)^{1/2}Q_{ea}, \tag{49}$$

$$\nu_{ei}=\frac{\alpha\rho}{m_a}\left(\frac{8kT}{\pi m_e}\right)^{1/2}Q_{ei}. \tag{50}$$

A curve fit from experimental results is employed for the electron-atom elastic cross section [31],

$$Q_{ea}=\begin{cases}(-0.35+0.775\times10^{-4}T)\times10^{-16}\ \ (\mathrm{cm}^2),\\ 10^4<T<5\times10^5\ \ \mathrm{K},\\ (0.39-0.551\times10^{-4}T+0.595\times10^{-8}T^2)\times10^{-16}\ \ (\mathrm{cm}^2),\\ T<10^4\ \ \mathrm{K},\end{cases} \tag{51}$$

while the Coulomb cross section is used for the electron-ion cross section,

$$Q_{ei}=\frac{2\pi e^4}{9k^2T^2}\ln\left(\frac{9k^3T^3}{4\pi e^6 n_e}\right). \tag{52}$$

The ionization frequency is given by

$$\nu_{\rm ion}=\frac{(1-\alpha)\rho}{m_a}K_f, \tag{53}$$

where K_f is the rate parameter for the ionization process and may be found in Hoffert and Lien [30] and references therein as

$$K_f=3.75\times10^{-16}T^{1.5}\left(\frac{E_a^1}{kT}+2\right)\exp\left(-\frac{E_a^1}{kT}\right)\ \ (\mathrm{cm}^3/\mathrm{sec}), \tag{54}$$

where E_a^1 is the energy of the first electronic level of argon. The reason for the appearance of the energy of the first excited state in the expression for the ionization frequency is as follows: As is discussed in [30], shock-tube experiments indicate that the collisional single ionization of argon takes place in two steps. In the first step, a free electron collides with an argon atom and excites it to its first electronic energy level. During the second stage, a collision of the excited atom with a free electron removes an electron from the excited state of the argon atom and by thus ionizes it. Furthermore, the experiments have shown that the entire ionization process is controlled by the first step, and hence it is its rate that is used to determine the ionization frequency.

Figure 4 presents the behavior of ν_ϵ and $\nu_{\rm ion}$ as functions of M_1 for $p_1=5$ Torr in argon. The solid curve corresponds to $2\nu_{\rm ion}$, while the dashed curve describes ν_ϵ. As can be seen, within the range $46<\theta<78$, $2\nu_{\rm ion}>\nu_\epsilon$, and hence in this range spontaneous emission may not take place. On the other hand, if, for example, the case of $\theta=30$ is examined, it is seen that only those waves whose frequencies are within

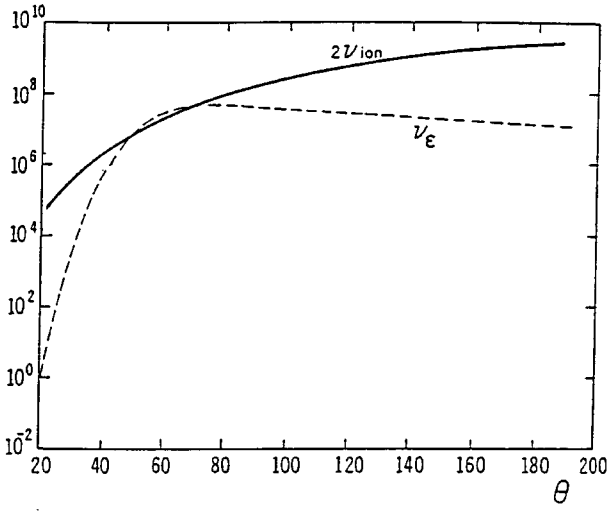

FIG. 4. The behavior of ν_ϵ (solid line) and $2\nu_{\rm ion}$ (dashed line) as functions of the temperature behind the shock for argon at $T=300$ K and $p_1=5$ Torr.

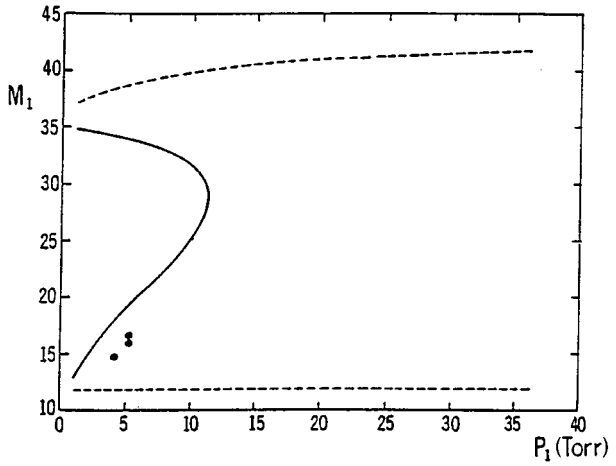

FIG. 5. Domains of spontaneous emission in the p_1-M_1 plane. In between the two dashed lines, $h>h_c$, while within the domain delimited by the solid line (along which $\nu_\epsilon=2\nu_{\rm ion}$) and the M_1 axis, $\nu_\epsilon\geqslant 2\nu_{\rm ion}$. The solid circles represent experiments cited in Glass and Liu [10], which exhibit irregular behavior behind the shock.

the range $10^3<\omega<10^5$ may be spontaneously emitted from the shock's front. To check whether this actually occurs, criterion (16) is employed together with Eqs. (45)–(47).

The results of the parametric studies are presented in Fig. 5. Along the two dashed lines $h=h_c$, while the equality $\nu_\epsilon=2\nu_{\rm ion}$ is satisfied along the solid line. Thus, inside the domain that is delimited by the solid line and the vertical axis, $2\nu_{\rm ion}\leqslant\nu_\epsilon$, and hence spontaneous acoustic emission may not occur for shocks whose propagation is represented in that domain. On the other hand, within the domain that lies between the two dashed lines, $h>h_c$. Therefore, spontaneous acoustic emission may occur for those shocks that are characterized by a pair of values (M_1,p_1) that is between the two dashed lines, but outside the solid curve. If, for example, the initial pressure is fixed at $p_1=5$ Torr and M_1 is raised, the shock starts to spontaneously emit sound as well as entropy-vortex waves with $\omega\gg\nu_\epsilon$ once M_1 becomes greater than 12. However, as the Mach number is raised beyond 18, the shock stabilizes as the spontaneous emission ceases due to entering into the domain in which local ionization equilibrium may not exist. Raising the Mach number still further results in leaving the latter domain and subsequently in the reoccurrence of spontaneous emission for $34<M_1<38$. However, a word of caution is due for that domain. At such high Mach numbers, effects such as second ionization may play an important role in determining the Hugoniot curve and subsequently in calculating the conditions for spontaneous emission. For example, the Hugoniot curve is expected to have two maxima if second ionization is taken into account and thus the slope of the Hugoniot curve may change sign in that range of Mach numbers.

The effect of the pressure ahead of the shock on the occurrence of spontaneous emission may be studied by varying it for a given Mach number. If the latter is fixed, say, at $M_1=15$, it is seen that for low values of p_1 the shock is stable under spontaneous emission. However, as the pressure ahead of the shock is raised beyond 2.5 Torr, the shock enters into the instability regime. Thus a general conclusion that my be drawn from Fig. 5 is that higher pressure ahead of the shock promotes instability under spontaneous emission. Such a tendency was indeed observed in Houwing *et al.* [13] who found that while shocks that propagated in neon with initial pressure of 5 Torr were stable, raising the initial pressure to 10 Torr and keeping the same Mach number resulted in instability.

The experiments of Glass and Liu [10] are shown by the solid circles in Fig. 5. In those experiments, irregular behavior was observed behind the shocks. As can be seen, the parameters of those experiments do indeed belong to the theoretical domain of spontaneous emission.

[1] C. Park, J. Thermophys. Heat Transfer **7**, 385 (1993).
[2] J. R. Maus, B. J. Griffith, and K. Y. Sgema, J. Spacecrafts **21**, 136 (1984).
[3] M. N. Macrosan, J. Fluid Mech. **217**, 167 (1990).
[4] M. A. Tsikulin and E. G. Popov, *Radiative Properties of Shock Waves in Gases* (Nauka, Moscow, 1986).
[5] G. A. Lukyanov, *Supersonic Plasma Jets* (Mashinostroenie, Moscow, 1985).
[6] *Shock Waves Marseille I, Hypersonics, Shock-Tube and Shock Tunnel Flow*, edited by R. Brun and L. Z. Domitrescu (Springer-Verlag, Berlin, 1995).
[7] V. A. Bronshten, Solar Syst. Res. **27**(1), 80 (1993).
[8] H. Nieuwenhuijzen, C. De Jager, C. Cuntz, M. Lobel, and L. Achmad, Astron. Astrophys. **280**, 195 (1993).
[9] C. F. McKee and B. T. Draine, Science **252**, 397 (1991).
[10] I. I. Glass and W. S. Liu, J. Fluid Mech. **84**, 55 (1978).
[11] I. I. Glass, W. S. Liu, and F. C. Tang, Can. J. Phys. **55**, 1269 (1977).
[12] R. W. Griffith, R. J. Sandeman, and H. G. Hornung, J. Phys. D **9**, 1681 (1976).
[13] A. F. P. Houwing, T. J. McIntyre, P. A. Taloni, and R. J. Sandeman, J. Fluid Mech. **170**, 319 (1986).
[14] T. J. McIntyre, A. F. P. Houwing, R. J. Sandeman, and H. A. Bachor, J. Fluid Mech. **227**, 617 (1991).
[15] S. P. Dyakov, Zh. Eksp. Teor. Fiz. **27**, 288 (1954).
[16] V. M. Kontorovich, Zh. Eksp. Teor. Fiz. **33**, 1525 (1957).
[17] V. M. Kontorovich, Sov. Phys. Acoust. **5**, 320 (1959).
[18] I. A. Alieva and E. A. Andreev, Sov. Phys. Tech. Phys. **32**, 686 (1987).
[19] A. S. Baryshnikov, N. Yu. Vasil'ev, and A. B. Stefanov, Combust., Explos. Shock Waves **23**, 93 (1987).
[20] A. G. Bashkirov, PMM **50**, 576 (1986).
[21] S. A. Egorushkin and V. S. Uspenskii, Fluid Dyn. (USSR) **25**, 435 (1990).
[22] M. Mond and I. Rutkevich, J. Fluid Mech. **275**, 121 (1994).
[23] H. Petcheck and S. Byron, Ann. Phys. (N.Y.) **1**, 270 (1957).
[24] P. E. Oettinger and D. Bershader, AIAA J. **5**, 1625 (1967).
[25] A. Kaniel, O. Igra, G. Ben-Dor, and M. Mond, Phys. Fluids **29**, 3618 (1986).
[26] M. Mitchner and C. H. Kruger, Jr., *Partially Ionized Gases*

(Wiley-Interscience, New York, 1973).
[27] K. S. Drellishak, D. P. Aeschliman, and A. B. Campbel, Phys. Fluids **6**, 1280 (1963).
[28] L. M. Biberman, V. S. Vorobjev, and I. T. Yakubov, *Kinetics of Non-Equilibrium Low Temperature Plasmas* (Plenum, New York, 1986).
[29] I. Rutkevich and M. Mond, J. Propul. Power **10**, 906 (1994).
[30] M. I. Hoffert and H. Lien, Phys. Fluids **10**, 1769 (1967).
[31] M. Y. Jaffrin, Phys. Fluids **6**, 24 (1961).